BIOCELL

Tech Science Press

Doi:10.32604/biocell.2025.062380

ARTICLE

Quercetin Alleviates the Inflammatory Response and Oxidative Stress of Myoblasts after Ischemia/Reperfusion by Inhibiting NOX-2

Fu-Ping Zhu[1,#], Wu-Ping Li[1,#], Yin-Sheng Cao[1], Zhen-Zhen Cai[1], Hang Wu[1], Yu-Tong Zhu[2,*] and Hui Liu[3,*]

[1]Department of Foot and Ankle Orthopedics, The First Hospital of Hunan University of Chinese Medicine, Changsha, 410007, China
[2]The First Clinical College of Traditional Chinese Medicine, Hunan University of Chinese Medicine, Changsha, 410208, China
[3]Department of Orthopedic Surgery, The Second Xiangya Hospital of Central South University, Changsha, 410011, China

*Corresponding Authors: Yu-Tong Zhu. Email: zhuyutong20223069@stu.hnucm.edu.cn;
Hui Liu. Email: huiliu568977908@163.com

[#]These authors, Fu-Ping Zhu and Wu-Ping Li, contributed equally to this work

Received: 17 December 2024; Accepted: 08 May 2025; Published: 24 June 2025

ABSTRACT: Objective: Limb ischemia-reperfusion injury (LIRI) may lead to tissue necrosis and loss of function, even life-threatening. Our previous study found that Tao-Hong-Si-Wu decoction (THSWD) had some efficacy in treating of LIRI. Quercetin, the major component of THSWD, was selected further to uncover the molecular mechanism underlying its treatment of LIRI. **Methods:** In this study, myoblasts were isolated from rat gastrocnemius muscle tissue, and an *in vitro* LIRI model was established. The cell counting kit-8 (CCK-8) and colony formation assay were used to evaluate the impact of quercetin on LIRI-induced myoblast viability and proliferation. Lactate dehydrogenase (LDH) activity was measured to detect myoblast injury in the LIRI model. The apoptosis of myoblasts was evaluated by Hoechst staining and flow cytometry. In addition, molecular docking analysis was performed to predict the interaction between quercetin and NADPH oxidase 2 (NOX-2). Subsequently, we investigated the molecular mechanism of quercetin in LIRI-induced myoblasts by overexpressing NOX-2. **Results:** The myogenic marker Desmin was highly expressed in isolated myoblasts. In the LIRI model, myoblast viability and proliferation were decreased, and cell injury and apoptosis levels were increased. In addition, NOX-2 was highly expressed in the LIRI model. At the same time, LIRI induction promoted the up-regulation of oxidative stress and inflammatory response. Quercetin significantly reversed the effects of LIRI treatment on myoblasts in a concentration-dependent manner. Molecular docking suggested an interaction between quercetin and NOX-2. Further overexpression of NOX-2 inhibited the effect of quercetin on LIRI-induced myoblasts. **Conclusion:** Quercetin could reduce inflammatory response and oxidative stress by inhibiting NOX-2, thus playing a therapeutic role in treating LIRI.

KEYWORDS: Quercetin; limb ischemia-reperfusion; myoblasts; NOX-2; inflammatory; oxidative stress

1 Introduction

Limb ischemia-reperfusion injury (LIRI) refers to the injury that occurs when the blood supply of the limb or tissue is restored after a period of ischemia [1]. Ischemia leads to cell hypoxia and accumulation of metabolites, which rapidly enter the ischemic region when blood flow is restored, leading to cell damage and the development of inflammatory responses. This can cause a series of pathophysiological changes, including cell damage, oxidative stress, inflammatory response, free radical production, and tumor necrosis factor release [2,3]. LIRI can lead to a variety of clinical manifestations, such as swelling, pain, dysfunction, spasms,

and gangrene. In severe cases, it can lead to tissue necrosis and loss of function, even life-threatening [4]. Studies have shown that LIRI mainly occurs in populations such as replantation of amputated limbs and crush injuries [5,6]. The incidence of LIRI is significantly increased when the limb ischemia time exceeds 6–8 h in the population with replantation of amputated limbs [7]. The mortality rate caused by LIRI is as high as 48% in the severe crush injury population [8]. At present, the treatment of LIRI mainly includes reperfusion control and fasciotomy. Reperfusion control can slow oxidative damage and inflammatory responses during reperfusion, but has limited efficacy in patients with severe LIRI. Fasciotomy can effectively reduce the pressure of reperfusion, but patients recover slowly and are prone to infection [5,9]. Therefore, we need to deeply investigate the pathogenesis of LIRI to provide new insights for its treatment.

Tao-Hong Si-Wu decoction (THSWD) is a commonly prescribed traditional Chinese medicine in clinical practice. Its composition included *Persicae Semen*, *Carthami Flos*, *Angelicae Sinensis Radix*, *Paeoniae Radix Alba*, *Chuanxiong Rhizoma*, and *Rehmanniae Radix Praeparata* [10]. THSWD can prevent and treat coronary heart disease, stroke, and other cardiovascular diseases [11]. Current research mechanisms show that THSWD can prevent and treat myocardial injury by inhibiting inflammatory response, anti-oxidative stress, anti-fibrosis, reducing blood lipids, anti-atherosclerosis, improving vascular pathological changes, and regulating related signaling pathways, so as to protect cardiomyocytes and improve cardiac function [11]. Our previous study showed that THSWD pretreatment reduced the secretion of proinflammatory cytokines TNF-α and IL-1β and reduced Ca^{2+} concentration in LIRI rats [6].

It is worth mentioning that quercetin has been confirmed to be one of the key active components of THSWD [10,12]. Quercetin is a flavonoid with diverse biological effects, including antioxidant, anti-cancer, anti-inflammatory, anti-aggregation, and anti-aging [13]. Given that inflammation and oxidative stress are the main drivers of I/R, quercetin has antioxidant and anti-inflammatory activities, which are beneficial in improving I/R [14]. The study by Lin et al. found that quercetin could effectively reduce tissue necrosis and inflammation induced by hepatic IRI [15]. In addition, quercetin has also been reported in the treatment of cerebral and renal ischemia. Quercetin enhances the protective effect against renal IRI by reducing lipid peroxidation and enhancing the antioxidant system [16]. Quercetin can treat cerebral IRI by promoting M2 polarization of microglia/macrophages [17]. However, the exact molecular mechanism by which quercetin treats LIRI has not yet been elucidated and requires further investigation.

NOX-2 is an enzyme that exists in a variety of cells [18]. Belonging to the NADPH oxidase family, this enzyme primarily facilitates electron transfer from the oxidoreductase NADPH to molecular oxygen, resulting in the production of reactive oxygen species (ROS) like superoxide anions [19]. Activation of NOX-2 can lead to heightened oxidative stress and inflammation, which in turn can further activate NOX-2, forming a positive feedback regulatory loop [20]. Moderate NOX-2 activation and oxidative stress can have a certain protective effect on the body. Still, excessive activation or persistence can cause inflammation and damage, which is correlated with the progression of various diseases [18,21,22]. Therefore, regulation of NOX-2 activity and oxidative stress status has great significance for the treatment and prevention of inflammation-related diseases. However, whether NOX-2 is involved in regulating LIRI progression is unknown.

To date, studies related to evaluating the efficacy of quercetin in LIRI have not been reported. Building on the research background, we dare to hypothesize that quercetin may regulate LIRI progression through NOX-2 signaling. In the present study, myoblasts were isolated from rat gastrocnemius muscle tissue, and an *in vitro* LIRI model was constructed. We aimed to explore the potential of quercetin to alleviate LIRI and its regulatory mechanism, which has important clinical significance for treating LIRI.

2 Materials and Methods

2.1 Extraction of Myoblasts

Healthy male Sprague-Dawley rats, 2 months of age, were obtained from Hunan SJA Laboratory Animal Co., Ltd. The environment of the experimental animals was kept constant temperature, constant humidity, quiet, and no harmful substances. The temperature and humidity are controlled according to the type of experimental animal and the experimental needs, generally 22°C–25°C and 40%–60% relative humidity. Illumination was generally a 12-h light cycle. The environment is clean, dust-free, and odor-free. After a one-week adaptation period, rat gastrocnemius tissue was harvested. Then the tissue samples were enzymatically digested using 1 mg/mL collagenase II (MCE, HY-E70005B, Shanghai, China) at 37°C for 30 min, ensuring complete submersion of the tissue fragments. The volume of collagenase II should submerge the tissue block. After purification, cells were seeded into F-10 complete medium (Pricella, PM151110B, Wuhan, China) supplemented with 10% fetal bovine serum (Gibco, 10099141, Grand Island, NY, USA) and 1% penicillin/streptomycin (Abiowell, AWH0529a, Changsha, China), then plated at a density of 2×10^5/well. Cell cultures were maintained in a humidified incubator (37°C, 5% CO_2, 95% air). The growth of gastrocnemius muscle cells was monitored under an inverted microscope (Cnmicro, DSZ2000X, Beijing, China). The primary cells were cultured for 3–6 passages and identified as myoblasts before subsequent experiments.

The animal experiments in this study were approved by the Animal Ethics Committee of the First Affiliated Hospital of Hunan University of Chinese Medicine (ZYFY20220228).

2.2 Immunofluorescence (IF)

The slides were fixed, and 0.3% Triton X-100 was added to permeate at 37°C for 30 min. Subsequently, 5% BSA-PBS (Solarbio, SW3015, Beijing, China) was added to the block for 60 min. Primary antibody Desmin (1:50) (Proteintech, 60226-1-Ig, Chicago, IL, USA) was added and incubated overnight at 4°C. 50~100 μL Goat anti-Mouse IgG (H+L) Secondary Antibody Alexa Fluor488 (1:200) (Abiowell, AWS0004c) was added dropwise at 37°C for 90 min. Then, nuclear staining was performed with DAPI solution (Abiowell, AWI0429) for 10 min in the dark. Finally, they were examined by fluorescence microscopy (Motic, BA210T, Xiamen, China).

2.3 Cell Treatment

The simulated ischemia-reperfusion solutions were prepared with reference to previous studies [6]. The principle is that by adjusting parameters such as potassium ion concentration, the electrolyte disorder caused by cell membrane rupture during ischemia *in vivo* can be simulated. The preparation of simulated ischemic solution: NaH_2PO_4 0.9 mmol/L, $NaHCO_3$ 6.0 mmol/L, $CaCl_2$ 1.8 mmol/L, $MgSO_4$ 1.2 mmol/L, sodium lactate 40 mmol/L, HEPES 20 mmol/L, NaCl 98.5 mmol/L, KCl 10.0 mmol/L, and natrium hydrosulfurosum 10 mmol/L, pH 6.8. The preparation of simulated reperfusion solution: NaCl 29.5 mmol/L, KCl 5 mmol/L, NaH_2PO_4 0.9 mmol/L, $NaHCO_3$ 20 mmol/L, $CaCl_2$ 1.8 mmol/L, $MgSO_4$ 1.2 mmol/L, HEPES 20 mmol/L, glucose 55 mmol/L, and pH 7.4. According to different experimental purposes, myoblasts can be grouped as Sham, LIRI, LIRI+Quercetin, LIRI+Quercetin+oe-NC, and LIRI+Quercetin+oe-NOX-2. In the Sham group, cells were cultured normally. In the LIRI group, cells were treated for 4 h in the ischemic solution and then for 8 h in the reperfusion solution [6]. In the LIRI+Quercetin group, the cells were treated with 10, 25, 50, 75, or 100 μM quercetin (MCE, HY-18085) for 24, 48, or 72 h before ischemia-reperfusion [6,23]. In the LIRI+Quercetin+oe-NC and the LIRI+Quercetin+oe-NOX-2 group, cells were transfected with oe-NC or

oe-NOX-2 (Honorgene, HG-HR023965, Changsha, China) for 6 h and then treated with 50 μM quercetin for 48 h before ischemia-reperfusion treatment. Quercetin was dissolved in DMSO.

2.4 Western Blot Analysis

Myoblast samples were collected and then lysed using RIPA buffer (Abiowell, AWB0136), followed by BCA kits (Abiowell, AWB0104) to quantify the protein concentration. Separated proteins were electrophoretically transferred to nitrocellulose membranes (Pall, PALL66485, New York, NY, USA). Membranes were blocked, followed by overnight incubation at 4°C with primary antibodies diluted in blocking buffer. After three washes, membranes were incubated with secondary antibodies for 90 min at room temperature. Nitrocellulose membranes were exposed to Super ECL Plus detection reagent (Abiowell, AWB0005). Band intensities were quantified with β-actin as an internal reference. Complete antibody information, including dilution ratios and commercial sources, is provided in Table 1.

Table 1: The information about antibodies

Name	Dilution rate	Cat number	Source	Company	Country
Desmin	1:1000	AWA00524	Mouse	Abiowell	China
Myogenin	1:200	ab124800	Rabbit	abcam	UK
MHC	1:2000	AWA10045	Rabbit	Abiowell	China
GAPDH	1:5000	10494-1-AP	Rabbit	Proteintech	USA
NOX-2	1:2000	AWA10048	Rabbit	Abiowell	China
p-p47phox	1:1000	ab74095	Rabbit	abcam	UK
p47phox	1:1000	ab308256	Rabbit	abcam	UK
p-p67phox	1:2000	PA5-105094	Rabbit	Thermo	USA
p67phox	1:10000	ab109523	Rabbit	abcam	UK
Rac1	1:1000	24072-1-AP	Rabbit	Proteintech	USA
β-actin	1:5000	66009-1-Ig	Mouse	Proteintech	USA
Goat anti-Rabbit IgG	1:5000	AWS0002	/	Abiowell	China
Goat anti-Mouse IgG	1:5000	AWS0001	/	Abiowell	China

2.5 Cell Counting Kit-8 (CCK-8) Assay

Cells were plated at a density of 5×10^3 cells/well and allowed to adhere. Following cell treatment, 10 μL CCK-8 reagent (DOJINDO, NU679, Kumamoto, Japan) was added according to the established time-course protocol. After replacing the treatment medium with 100 μL fresh medium containing CCK-8, plates were incubated for 4 h at 37°C. The optical density (OD) at 450 nm was measured using a microplate reader (HEALES, MB-530, Shenzhen, China).

2.6 Colony Formation Assay

Clone formation assay was performed to evaluate myoblast proliferative capacity. Cells in the exponential growth phase were digested with 0.25% trypsin and mechanically dissociated into single-cell suspensions. Then, myoblasts were suspended in a complete medium with 10% fetal bovine serum. A standardized density of 200 viable cells/well was plated into 6-well culture plates to ensure uniform distribution. The cultures were maintained under standard conditions (37°C, 5% CO_2) for 14 days with medium replacement every 72 h. Cultures were terminated when macroscopic clones appeared in the dish. After myoblasts were fixed, cells

were stained with 1 mL Crystal Violet (Abiowell, AWC0333a). The staining solution was slowly washed off and then dried naturally and photographed for recording.

2.7 Detection of Oxidative Stress Indicators

The content of lactate dehydrogenase (LDH) in myoblasts was detected according to the kit instruction (njjcbio, A020-2, Nanjing, China) to evaluate the degree of cell membrane damage [24]. Finally, the OD at 450 nm was measured.

The contents of superoxide dismutase (SOD) (njjcbio, A001-3), catalase (CAT) (njjcbio, A007-1-1) and malondialdehyde (MDA) (njjcbio, A003-1) in myoblasts were detected to evaluate the oxidative stress level of cells. Finally, the OD values were measured at 450, 405, and 532 nm by microplate reader (HEALES, MB-530), respectively.

The generation of intracellular ROS was determined using a ROS assay kit (Beyotime, S0033S, Nanjing, China). Myoblasts and DCHF-DA reagent were co-incubated for 20 min in a cell culture incubator. The intracellular fluorescence intensity was assessed by a flow cytometer (Beckman Coulter, A00-1-1102, Brea, CA, USA).

2.8 Hoechst-Propidium Iodide (PI) Staining

Myoblast apoptosis was detected using the relevant kit (Abiowell, AWC0304a). After the medium was removed, 5 μL Hoechst 33342 Stain and 5 μL PI Stain were added and incubated for 20–30 min at 4°C. Observations were made immediately after cleaning.

2.9 Flow Cytometry

Cell apoptosis was analyzed using an Annexin V-APC/PI kit (KeyGEN BioTECH, KGA1030, Nanjing, China). In brief, myoblasts were collected by digestion with trypsin without EDTA. Then, the cells were suspended. Cells were dual-stained with 5 μL Annexin V-APC and 5 μL PI were added, followed by 10 min dark incubation at room temperature. Finally, the analysis was performed by flow cytometry (Beckman Coulter, A00-1-1102).

2.10 Real-Time Quantitative Polymerase Chain Reaction (RT-qPCR)

Total RNA was extracted from myoblasts using the Trizol reagent (Thermo, 15596026, Waltham, MA, USA). RNA quality was verified spectrophotometrically (OD260/280 ratio 1.8–2.0) prior to reverse transcription. RT-qPCR was conducted using QuantStudio1 Real-Time PCR System (ABI, Carlsbad, CA, USA) with UltraSYBR Mixture (CWBIO, CW2601, Taizhou, China). The relative gene expression was analyzed using the $2^{-\Delta\Delta Ct}$ method, normalized to β-actin as endogenous control. Primer sequences information is detailed in Table 2. All reactions included no-template controls and were performed in technical triplicate.

Table 2: The primer sequences used in the study were listed

Targets	F (5′-3′)	R (5′-3′)	Accession no.	Size (bp)
R-NOX-2	TGCAGCCAAATGC CCTGATA	AAGGCGCTCTGAA ACCATGA	66021	151
R-Rac1	AGCCATGGCGAA AGAGATCG	AACGGCTCGGA TAGCTTCAT	363875	100

(Continued)

Table 2 (continued)

Targets	F (5′-3′)	R (5′-3′)	Accession no.	Size (bp)
R-p47phox	AGAGTCATCCCT CACCTCCC	GAGATCTTCACGG GCAGTCC	114553	119
R-p67phox	AAGTCTGAGCCC AGGCATTC	CCGTAGCCTTGCC CAGATAG	364018	160
R-β-actin	ACATCCGTAAAGACC TCTATGCC	TACTCCTGCTTGCT GATCCAC	81822	223

2.11 Molecular Docking

The structures of the NOX-2 protein and the quercetin molecular were downloaded from the ProteinData Bank (https://www.rcsb.org/) and the PubChem database (https://pubchem.ncbi.nlm.nih.gov/), respectively. Molecular docking analysis was performed using Autodock Vina 1.5.6 (The Scripps Research Institute, La Jolla, CA, USA) and PYMOL 3.0.3 (Schrödinger, New York, NY, USA). In brief, proteins were treated, such as dehydration and removal of organic matter. The protein hydrogenation and other processing were performed, followed by searching for the appropriate protein active site [25].

2.12 Enzyme-Linked Immunosorbent Assay (ELISA)

Myoblasts were centrifuged at 500× *g* for 5 min at 2°C–8°C, and then the supernatant was collected. The corresponding indicators were detected using Interleukin-6 (IL-6) (Proteintech, KE20024), Interleukin-1β (IL-1β) (Proteintech, KE20021), and Tumor necrosis factor-*α* (TNF-*α*) (Proteintech, KE20018) kits according to the manufacturer's instructions. Finally, OD values were measured at 450 nm using a microplate reader (HEALES, MB-530).

2.13 Statistical Analysis

All experimental data were analyzed using GraphPad Prism 8.0 (GraphPad Software, San Diego, CA, USA) and presented as mean ± standard deviation from triplicate independent experiments. The normality assumption was verified using Shapiro-Wilk testing. Comparisons between multiple groups were performed using the One-way ANOVA test with Tukey's post hoc test. Statistical significance was defined as $p < 0.05$.

3 Results

3.1 Identification of Primary Myoblasts

Myoblasts were cultured for 3–6 passages and then examined for cell morphology by light microscopy. Compared with the cells cultured in the second passage (P2), the cells cultured in the fourth passage (P4) were striated (Fig. 1A), and this morphology was consistent with typical myoblast characteristics [6]. In addition, WB results showed that the expressions of myogenic markers Desmin, myogenin (MYOG), and myosinheavy chain (MHC) in myoblasts were significantly increased in P4 myoblast compared with P2 myoblast (Fig. 1B). Meanwhile, IF results showed that Desmin expression was detected in the P4 myoblast (Fig. 1C). Flow cytometry showed that MyOD+CD45- ≥ 95% in the P4 myoblast (Fig. 1D). The above results indicated that the isolation of myoblasts from rat gastrocnemius muscle tissue was successful.

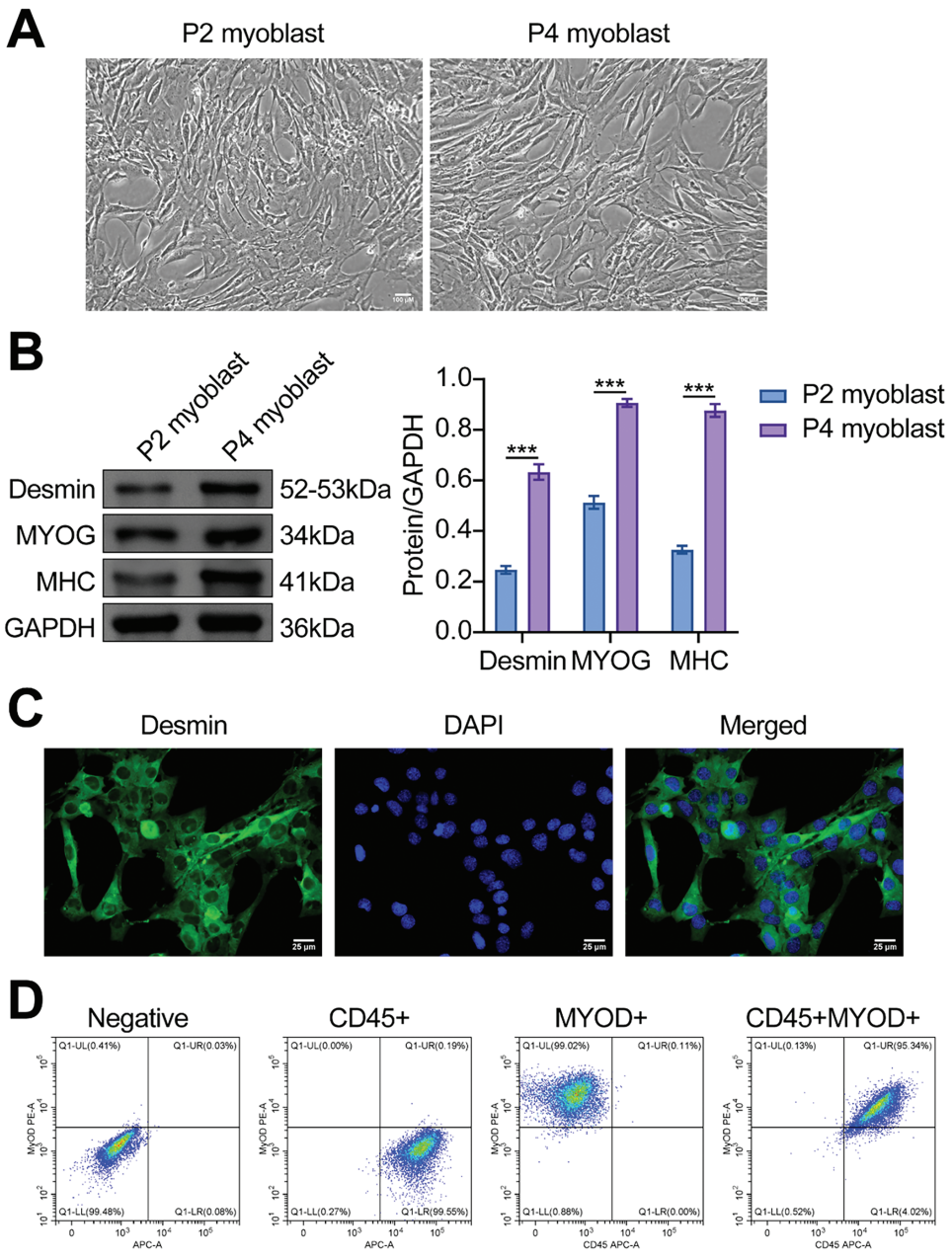

Figure 1: Identification of primary myoblasts. (**A**) The morphology of myoblasts was observed by a light microscope. Scale bar = 100 μm. (**B**) The protein expressions of myogenic markers (Desmin, MYOG, and MHC) in the second and fourth-generation myoblasts were detected. (**C**) IF was used to detect Desmin expression in myoblasts. Scale bar = 25 μm. (**D**) The expressions of the myoblast markers MyOD and CD45 in the P4 cells were verified using flow cytometry. ***$p < 0.001$. The number of repetitions (n) = 3

3.2 Quercetin Alleviated LIRI-Induced Decline in Myoblast Viability

Next, we evaluated the effect of quercetin on myoblast viability in the LIRI model. As shown in Fig. 2A, LIRI-induced myoblast viability was significantly increased after quercetin treatment. The treatment effect of quercetin for 48 and 72 h was better. However, cell viability began to decrease at 75 μM concentration.

Then, the clone formation assays revealed a notable decrease in myoblast proliferation levels in the LIRI group as opposed to the Sham group. Conversely, there was a concentration-dependent elevation in myoblast proliferation levels following treatment with 10, 25, and 50 μM of quercetin (Fig. 2B). In addition, the LDH results indicated that quercetin significantly ameliorated LIRI damage to the cell membrane (Fig. 2C). By Hoechst staining, we could observe that the nuclei cells in the Sham group showed regular contours with round or oval shapes. In contrast, many cells in the LIRI group were observed to have smaller nuclei and condensed chromatin. At the same time, the addition of varying concentrations of quercetin improved the nuclear morphological features and decreased the number of apoptotic cells (Fig. 2D). Flow results further verified that quercetin significantly inhibited apoptosis in myoblasts (Fig. 2E). Taken together, the above evidence suggested that quercetin could effectively alleviate LIRI-induced decline in myoblast viability.

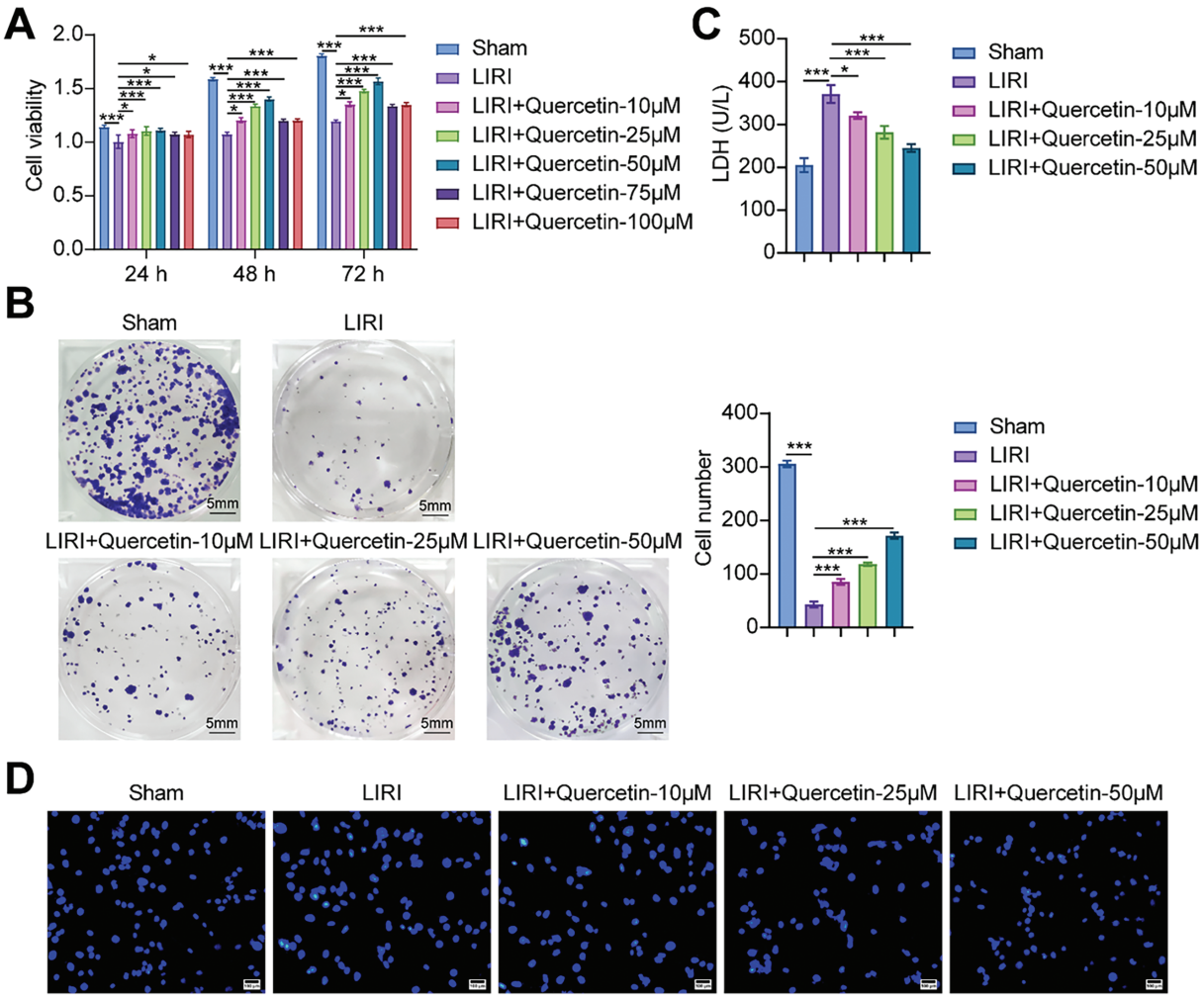

Figure 2: (Continued)

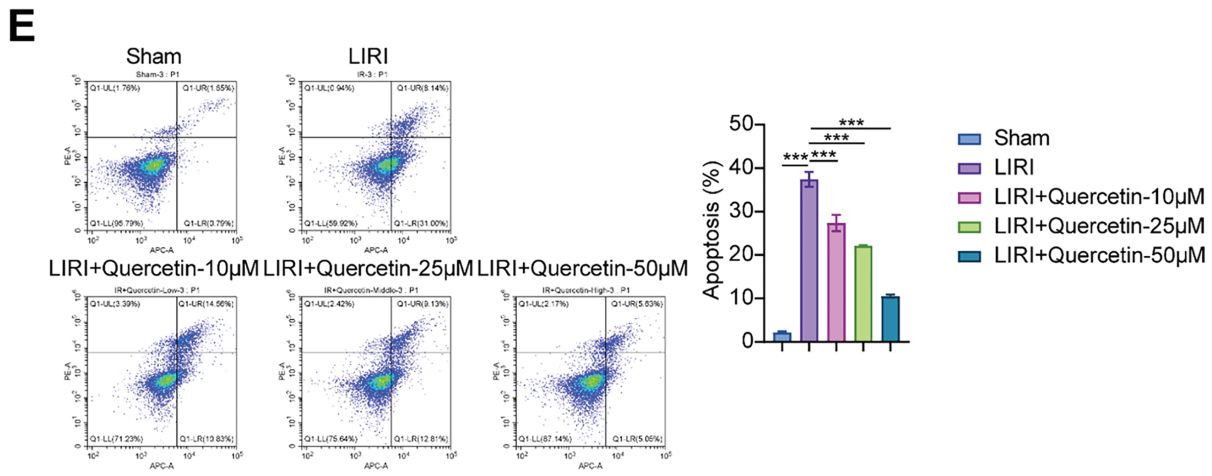

Figure 2: Quercetin alleviated LIRI-induced decline in myoblast viability. (**A**) Myoblast viability was measured by CCK-8 assay. (**B**) Myoblast proliferation was evaluated using a colony formation assay. Scale bar = 5 mm. (**C**) LDH activity in myoblasts was detected to evaluate the degree of cell membrane damage. (**D**,**E**) Hoechst staining and flow cytometry were used to assess the level of myoblast apoptosis. Scale bar = 100 μm. $^{*}p < 0.05$, $^{***}p < 0.001$. $n = 3$

3.3 Quercetin Inhibited LIRI-Induced Inflammatory Response and Oxidative Stress in Myoblasts

RT-qPCR and Western blot analyses demonstrated that NOX-2 was highly expressed in the LIRI model. Notably, quercetin decreased NOX-2 expression in a concentration-dependent manner (Fig. 3A). In order to verify whether there was a link between quercetin and NOX-2, molecular docking was performed. The binding energy of molecular docking was −9.4 kcal/mol, which was less than −5 kcal/mol. The molecular docking analysis suggested that quercetin could attach to the NOX-2 protein well on its own. Quercetin interacted with the amino acids and was stably bound to the NOX-2 protein's cavity, according to visual analysis performed with PYMOL (Fig. 3B). Previous studies showed that NOX-2 was an important factor in regulating cellular inflammation and oxidative stress [26,27]. We assessed the impact of quercetin on inflammatory response and oxidative stress in myoblasts. Fig. 3C showed that the levels of IL-6, TNF-α, and IL-1β were highly increased in the LIRI group. After the cells were treated with quercetin, the levels were notably reduced. Conversely, SOD and CAT exhibited significantly diminished levels, while the oxidative stress markers MDA and ROS showed significant elevation in the LIRI group. However, quercetin was effective in reducing oxidative stress in myoblasts (Fig. 3D,E). Systematic evaluation of quercetin's anti-inflammatory and antioxidant efficacy in myoblasts revealed dose-dependent modulation of stress pathways. In summary, our results demonstrated that quercetin could reduce inflammatory response and oxidative stress in LIRI-induced myoblasts.

3.4 Overexpression of NOX-2 Reversed the Protective Effect of Quercetin on LIRI-Induced Myoblast Viability

To explore the NOX-2 effect on the viability of myoblasts under LIRI conditions, we transfected oe-NOX-2 and its negative control into myoblasts. In the LIRI+Quercetin+oe-NOX-2 group, the viability and proliferation level of myoblasts were lower than those in the LIRI+Quercetin+oe-NC group (Fig. 4A,B). In addition, overexpression of NOX-2 significantly increased the levels of LDH and apoptosis (Fig. 4C–E). It was not difficult to find that overexpression of NOX-2 partially reversed the promoting effect of quercetin on LIRI-induced viability of myoblast.

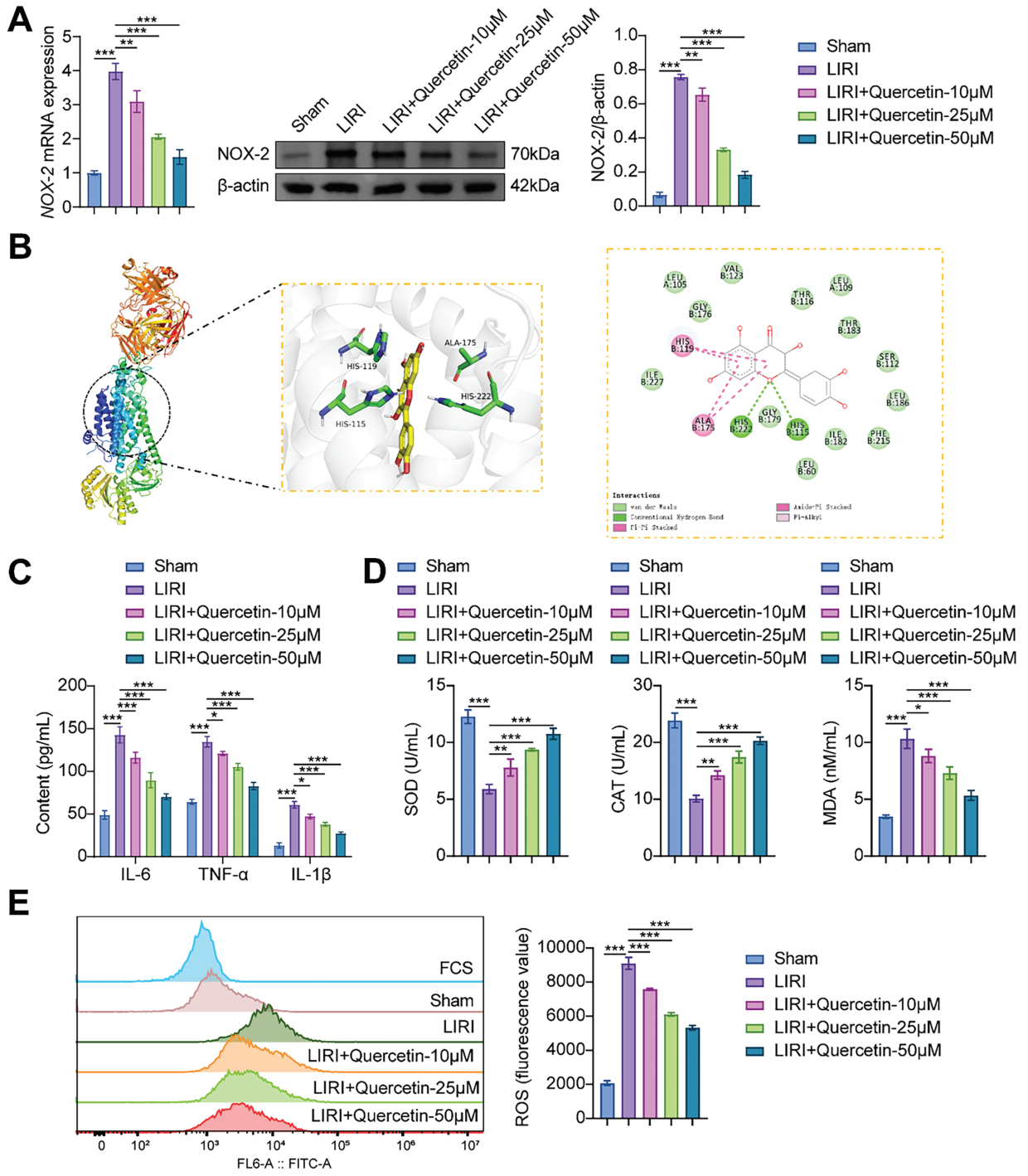

Figure 3: Quercetin inhibited LIRI-induced inflammatory response and oxidative stress in myoblasts. (**A**) The mRNA and protein expression of NOX-2 in myoblasts was detected. (**B**) The binding of quercetin to NOX-2 was verified by molecular docking. (**C**) Inflammatory factors (IL-6, TNF-α, and IL-1β) contents were determined through ELISA. (**D**) The levels of SOD and CAT activities, along with the MDA content in myoblasts, were measured by specific assay kits. (**E**) Flow cytometry was utilized to measure the ROS level. $^{*}p < 0.05$, $^{**}p < 0.01$, $^{***}p < 0.001$. $n = 3$

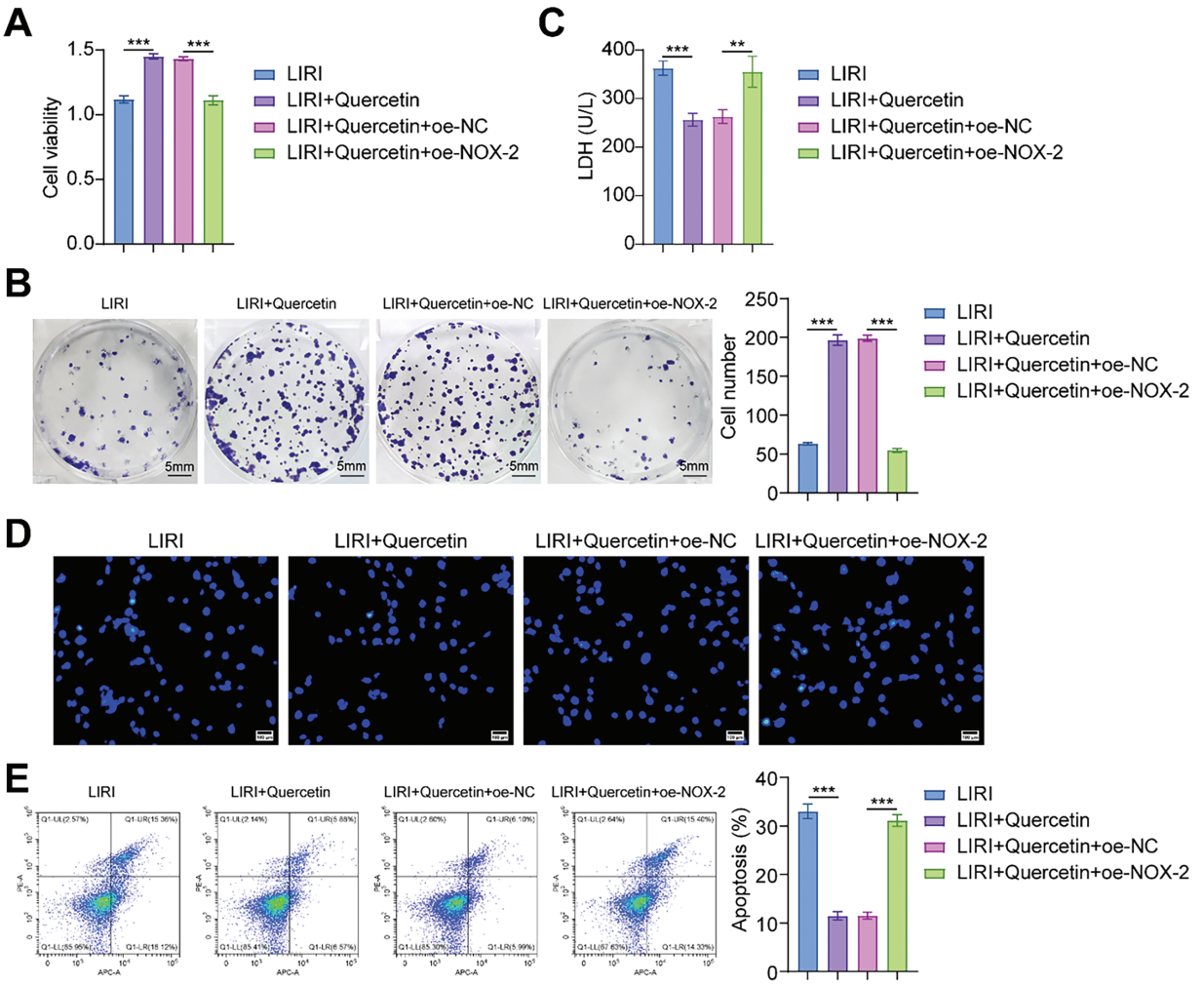

Figure 4: Overexpression of NOX-2 reversed the protective effect of quercetin on LIRI-induced myoblast viability. (**A**) The cell viability of myoblasts was assessed. (**B**) The degree of myoblast proliferation was determined through a colony formation assay. Scale bare = 5 mm. (**C**) LDH activity in myoblasts was measured using a kit assay. (**D**, **E**) Myoblast apoptosis was assessed by Hoechst staining and flow cytometry. Scale bar = 100 μm. $^{**}p < 0.01$, $^{***}p < 0.001$. $n = 3$

3.5 Overexpression of NOX-2 Reversed the Inhibitory Effects of Quercetin on LIRI-Induced Inflammation and Oxidative Stress in Myoblasts

Drawing from the aforementioned investigations, our hypothesis posits that quercetin could potentially modulate the LIRI-induced inflammatory responses and oxidative stress in myoblasts via NOX-2. As expected, the expression level of NOX-2 was elevated in myoblasts transfected with oe-NOX-2. Studies have shown that p47phox, p67phox, and Rac1 are the downstream factors of NOX-2 [28–30]. The overexpression of NOX-2 elevated mRNA expressions of Rac1, p47phox, and p67phox, as well as protein expression of Rac1, p-p47phox, and p-p67phox (Fig. 5A). Compared with the LIRI+Quercetin+oe-NC group, overexpression of NOX-2 increased the levels of IL-6, TNF-α, and IL-1β (Fig. 5B). These results further verified that NOX-2 promoted the inflammatory responses. In addition, the ctivities of SOD and CAT exhibited a substantial reduction, while the levels of MDA and ROS showed a significant increase in the LIRI+Quercetin+oe-NOX-2 group (Fig. 5C,D). These findings suggest that the overexpression of NOX-2 partially counteracted the

inhibitory impact of quercetin on oxidative stress. Collectively, these results imply that quercetin may confer a therapeutic benefit on LIRI-induced myoblasts by suppressing NOX-2 expression.

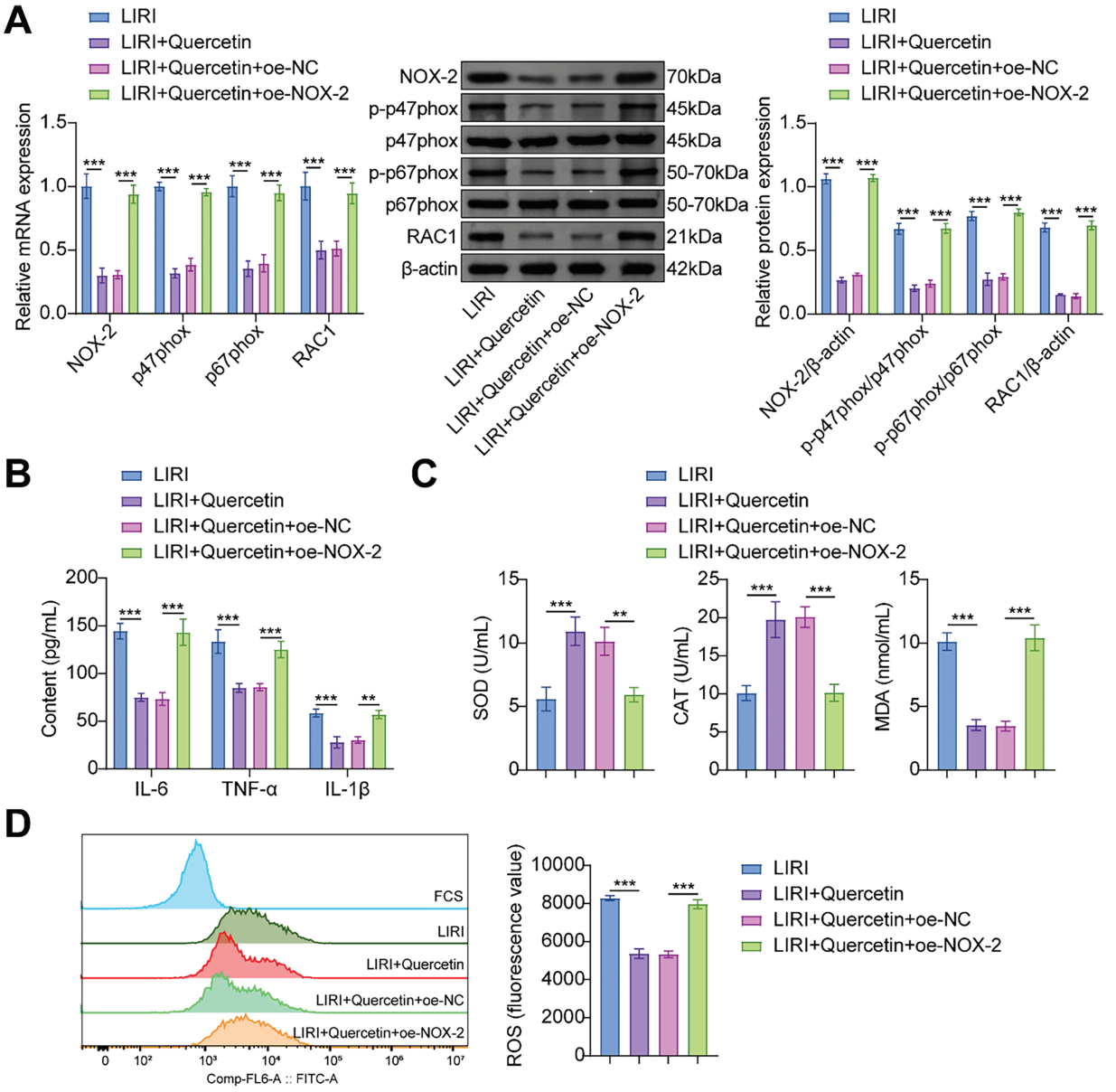

Figure 5: Overexpression of NOX-2 reversed the inhibitory effects of quercetin on LIRI-induced inflammation and oxidative stress in myoblasts. (**A**) The expression level of NOX-2, Rac1, p47phox, and p67phox in myoblasts was analyzed. (**B**) The contents of IL-6, TNF-α, and IL-1β were evaluated through ELISA. (**C**) The activities of SOD and CAT, along with the measurement of MDA content in myoblasts, were conducted using specific assay kits. (**D**) Flow cytometry was employed to determine the ROS level in the myoblasts. $^{**}p < 0.01$, $^{***}p < 0.001$. $n = 3$

4 Discussion

Acute lower limb ischemia is a prevalent vascular condition characterized by high morbidity and a grim prognosis. While the re-establishment of blood flow to the ischemic tissues is crucial for restoring

organ function, paradoxically, reperfusion therapy is linked to potential harm and, in some cases, exacerbates tissue damage [31,32]. Research indicates that oxidative stress plays a crucial role in I/R injury by causing an excessive production of oxygen free radicals and compromising antioxidant defenses, thereby significantly impacting cellular function [33]. ROS was implicated in the aggregation of platelets and granulocytes within microvessels, contributing to the development of microcirculatory abnormalities [34]. Furthermore, Drefs et al. showed that heightened ROS levels can impede the reperfusion process in ischemic tissues, leading to damage to cellular components and initiating endothelial cell death [35]. In this study, we successfully extracted myoblasts from rat gastrocnemius muscle tissue and constructed an LIRI myoblast model. In the LIRI model, we observed a marked increase in cell membrane damage, nuclear shrinkage, and an increased number of apoptotic cells in myoblasts. At the same time, SOD and CAT activities were significantly decreased, and MDA and ROS levels were increased in the LIRI group. Studies have shown that cells accumulate significant levels of xanthine oxidase substrates during ischemic injury, leading to the rapid production of superoxide anions and hydroxyl radicals upon reperfusion [36,37]. In addition, our data may further validate the idea that oxygen radicals oxidize membrane lipids within the phospholipid bilayer structure of the cell membrane, resulting in damage to the cell membrane and mitochondria. This oxidative damage can potentially activate various mechanisms of cell death [38,39]. In summary, our data further validate that cell death induced by I/R was closely related to oxidative stress.

Oxidative stress has been shown to be a decisive factor in the pathogenesis and advancement of I/R injury [33,40]. Still, a previous study showed that quercetin inhibited oxidative stress, and its therapeutic efficacy was demonstrated in animal models of I/R injury [41]. Quercetin is a potent scavenger of free radicals, especially for ROS [42,43]. Chen et al. demonstrated that quercetin protected cardiomyocytes from I/R injury by decreasing the activity of intracellular ROS-producing enzymes and inhibiting the expression of inflammatory mediators [44]. In our study, we verified the protective effect of quercetin on LIRI myoblasts. Treatment of LIRI myoblasts with quercetin resulted in an increase in myoblast viability and a significant decrease in the level of apoptosis. In addition, quercetin effectively inhibited the expression levels of IL-6, TNF-α, and IL-1β and reduced the oxidative damage of myoblasts. It was consistent with the findings of Ekinci Akdemir et al. Quercetin protected against I/R-induced oxidative damage in rats by decreasing MDA levels and increasing CAT activity [45]. Based on the above results, it is not difficult to find that quercetin may play a protective role in LIRI by inhibiting inflammatory responses and oxidative stress levels.

In this study, the interaction between quercetin and NOX-2 was confirmed by molecular docking analysis. NOX-2 was highly expressed in the LIRI model. We overexpressed NOX-2 in myoblasts to explore the role of NOX-2 in the treatment of LIRI with quercetin. Our results showed that overexpression of NOX-2 reduced the level of myoblast viability and proliferation, and the level of apoptosis was significantly increased. These results indicated that quercetin improved myoblast viability by inhibiting NOX-2 expression. Previous studies reported quercetin increased the cell viability and reduced the level of inflammation and cell death in the LPS-treated rat myocardial cell line H9C2 through NOX-2-related pathways [46]. Oxidative stress caused by the production of ROS played a major role in the inflammatory process. A study showed that quercetin could prevent LPS-induced oxidative stress and inflammatory response by regulating NOX-2/ROS/NF-KB signaling in lung epithelial cells [47]. This was consistent with our results. We found that quercetin could significantly inhibit ROS level and exert inhibitory effects on myoblast inflammation and oxidative stress through NOX-2 signaling. In addition to the NOX-2 signaling pathway. In addition, quercetin indirectly affected the binding of miR-485-5p to the YAP1 mRNA sequence by upregulating miR-485-5p expression, thereby regulating high glucose-induced and inflammatory response and oxidative stress [48]. Quercetin acts as a therapeutic agent to activate the NRF2/KEAP1 pathway to reduce lung ischemia-reperfusion injury [49].

In conclusion, our study elucidated the protective effects of quercetin on LIRI-induced myoblasts and the regulation mechanisms.

It is worth mentioning that there are still some limiting issues in this study. The outcomes of this study were obtained using the LIRI myoblast model, which may not completely capture the intricate and diverse features of human LIRI patients. Hence, it is imperative to combine animal studies and clinical data to confirm the therapeutic effect of quercetin on LIRI. Despite the promising therapeutic potential of quercetin in mitigating LIRI, a thorough investigation into its side effects and toxicity profile is crucial before considering its clinical utilization. Quercetin molecules may limit efficacy due to low solubility, instability, and bioavailability issues. All these questions are worthy of further exploration in future research. We can try to use liposomes or nanoparticle encapsulation to improve drug solubility and stability [50]. Drug water solubility and resistance to enzymatic hydrolysis can be enhanced by chemical modification [51]. More details are needed in combination with clinical trials to determine the best regimen. Additionally, the protective effect of quercetin on LIRI may be synergistic in multiple dimensions. Quercetin can inhibit the expression of autophagy-related proteins Beclin-1 and LC3-II and reduce the inflammatory response [52]. Quercetin can improve the microcirculation disorder after blood flow recanalization by improving the deformability of red blood cells [53]. These mechanisms may also apply to skeletal muscle and vascular endothelial cell protection in LIRI. Future studies can further explore the role of these mechanisms in LIRI and provide a basis for optimizing treatment regimens.

In short, the present study successfully established a LIRI-induced injury model of myoblasts, revealing the multiple protective effects of quercetin through targeted inhibition of NOX-2 expression. On the one hand, quercetin significantly enhanced cell viability and reduced the oxidative stress and inflammatory response induced by LIRI. On the other hand, mechanistic studies have shown that NOX-2 is a central driver of the oxidative inflammatory cascade in LIRI, and its overexpression partially counteracts the cytoprotective effects of quercetin. This finding is the first to elucidate the molecular mechanism by which quercetin improves myoblast function by regulating the NADPH oxidase pathway.

5 Conclusion

Our results suggested that quercetin targets NOX-2. Quercetin reduced the inflammatory and oxidative responses in LIRI-induced myoblasts by inhibiting the expression of NOX-2. Quercetin could effectively reduce the apoptosis level of myoblasts and enhance their survival ability. Our results enriched the rationale for the clinical use of quercetin for LIRI treatment.

Acknowledgement: Not applicable.

Funding Statement: This work was supported by National Natural Science Foundation of China (Grant 82274541 & 81674008), Key Project of Hunan Provincial Health Commission (Grant 202204072465) and Natural Science Foundation of Hunan Province (Grant 2020JJ4070).

Author Contributions: The authors confirm contribution to the paper as follows: study conception and design: Wu-Ping Li, Fu-Ping Zhu, Hui Liu; data collection: Fu-Ping Zhu, Hui Liu, Yin-Sheng Cao, Hang Wu, Zhen-Zhen Cai; analysis and interpretation of results: Fu-Ping Zhu, Wu-Ping Li, Yu-Tong Zhu; draft manuscript preparation: Fu-Ping Zhu, Wu-Ping Li. All authors reviewed the results and approved the final version of the manuscript.

Availability of Data and Materials: The datasets generated and/or analyzed during the current study are available from the corresponding author on reasonable request.

Ethics Approval: The animal experiments in this study were approved by the Animal Ethics Committee of the First Affiliated Hospital of Hunan University of Chinese Medicine (ZYFY20220228).

Conflicts of Interest: The authors declare no conflicts of interest to report regarding the present study.

References

1. Mi L, Zhang Y, Xu Y, Zheng X, Zhang X, Wang Z, et al. HMGB1/RAGE pro-inflammatory axis promotes vascular endothelial cell apoptosis in limb ischemia/reperfusion injury. Biomed Pharmacother. 2019;116(7):109005. doi:10.1016/j.biopha.2019.109005.
2. Zang X, Zhou J, Zhang X, Han Y, Chen X. Ischemia reperfusion injury: opportunities for nanoparticles. ACS Biomater Sci Eng. 2020;6(12):6528–39. doi:10.1021/acsbiomaterials.0c01197.
3. Simon F, Oberhuber A, Floros N, Busch A, Wagenhäuser MU, Schelzig H, et al. Acute limb ischemia-much more than just a lack of oxygen. Int J Mol Sci. 2018;19(2):374. doi:10.3390/ijms19020374.
4. Kim JH, Kim YC, Nahm FS, Lee PB. The therapeutic effect of vitamin C in an animal model of complex regional pain syndrome produced by prolonged hindpaw ischemia-reperfusion in rats. Int J Med Sci. 2017;14(1):97–101. doi:10.7150/ijms.17681.
5. McNally MM, Univers J. Acute limb ischemia. Surg Clin N Am. 2018;98(5):1081–96.
6. Fuping Z, Wuping L, Linhua W, Chengxi P, Fuqiang Z, Yi Z, et al. Tao-Hong-Si-Wu decoction reduces ischemia reperfusion rat myoblast cells calcium overloading and inflammation through the Wnt/IP3R/CAMKII pathway. J Cell Biochem. 2019;120(8):13095–106. doi:10.1002/jcb.28582.
7. Zhang L, Ipaktchi R, Ben Brahim B, Arenas Hoyos I, Jenni H, Dietrich L, et al. Prolongation of the time window from traumatic limb amputation to replantation from 6 to 33 h using *ex vivo* limb perfusion. Mil Med. 2024;189(S3):83–92. doi:10.1093/milmed/usae043.
8. Usuda D, Shimozawa S, Takami H, Kako Y, Sakamoto T, Shimazaki J, et al. Crush syndrome: a review for prehospital providers and emergency clinicians. J Transl Med. 2023;21(1):584. doi:10.1186/s12967-023-04416-9.
9. Apichartpiyakul P, Shinlapawittayatorn K, Rerkasem K, Chattipakorn SC, Chattipakorn N. Mechanisms and interventions on acute lower limb ischemia/reperfusion injury: a review and insights from cell to clinical investigations. Ann Vasc Surg. 2022;86:452–81. doi:10.1016/j.avsg.2022.04.040.
10. Chen J, Ye W. Molecular mechanisms underlying Tao-Hong-Si-Wu decoction treating hyperpigmentation based on network pharmacology, Mendelian randomization analysis, and experimental verification. Pharm Biol. 2024;62(1):296–313. doi:10.1080/13880209.2024.2330609.
11. Shao CL, Cui GH, Guo HD. Effects and mechanisms of taohong siwu decoction on the prevention and treatment of myocardial injury. Front Pharmacol. 2022;13:816347. doi:10.3389/fphar.2022.816347.
12. Liu TH, Chen WH, Chen XD, Liang QE, Tao WC, Jin Z, et al. Network pharmacology identifies the mechanisms of action of TaohongSiwu decoction against essential hypertension. Med Sci Monit. 2020;26:e920682. doi:10.12659/msm.920682.
13. Zhang YM, Zhang ZY, Wang RX. Protective mechanisms of quercetin against myocardial ischemia reperfusion injury. Front Physiol. 2020;11:956. doi:10.3389/fphys.2020.00956.
14. Pei B, Yang M, Qi X, Shen X, Chen X, Zhang F. Quercetin ameliorates ischemia/reperfusion-induced cognitive deficits by inhibiting ASK1/JNK3/caspase-3 by enhancing the Akt signaling pathway. Biochem Biophys Res Commun. 2016;478(1):199–205. doi:10.1016/j.bbrc.2016.07.068.
15. Lin J, Li F, Jiao J, Qian Y, Xu M, Wang F, et al. Quercetin, a natural flavonoid, protects against hepatic ischemia-reperfusion injury via inhibiting Caspase-8/ASC dependent macrophage pyroptosis. J Adv Res. 2025;70(2):555–69. doi:10.1016/j.jare.2024.05.010.
16. Gholampour F, Sadidi Z. Hepatorenal protection during renal ischemia by quercetin and remote ischemic perconditioning. J Surg Res. 2018;231:224–33. doi:10.1016/j.jss.2018.05.036.
17. Li L, Jiang W, Yu B, Liang H, Mao S, Hu X, et al. Quercetin improves cerebral ischemia/reperfusion injury by promoting microglia/macrophages M2 polarization via regulating PI3K/Akt/NF-κB signaling pathway. Biomed Pharmacother. 2023;168(10):115653. doi:10.1016/j.biopha.2023.115653.
18. Diebold BA, Smith SM, Li Y, Lambeth JD. NOX2 as a target for drug development: indications, possible complications, and progress. Antioxid Redox Signal. 2015;23(5):375–405. doi:10.1089/ars.2014.5862.

19. Wrublewsky S, Glas J, Carlein C, Nalbach L, Hoffmann MDA, Pack M, et al. The loss of pancreatic islet NADPH oxidase (NOX)2 improves islet transplantation. Redox Biol. 2022;55(3):102419. doi:10.1016/j.redox.2022.102419.
20. Singel KL, Segal BH. NOX2-dependent regulation of inflammation. Clin Sci. 2016;130(7):479–90. doi:10.1042/cs20150660.
21. Ardizzone A, Capra AP, Repici A, Lanza M, Bova V, Palermo N, et al. Rebalancing NOX2/Nrf2 to limit inflammation and oxidative stress across gut-brain axis in migraine. Free Radic Biol Med. 2024;213(11):65–78. doi:10.1016/j.freeradbiomed.2024.01.018.
22. Wu H, Wang Y, Zhang Y, Xu F, Chen J, Duan L, et al. Breaking the vicious loop between inflammation, oxidative stress and coagulation, a novel anti-thrombus insight of nattokinase by inhibiting LPS-induced inflammation and oxidative stress. Redox Biol. 2020;32(5):101500. doi:10.1016/j.redox.2020.101500.
23. Dungan CM, Murach KA, Zdunek CJ, Tang ZJ, Nolt GL, Brightwell CR, et al. Deletion of SA β-Gal+ cells using senolytics improves muscle regeneration in old mice. Aging Cell. 2022;21(1):e13528. doi:10.1111/acel.13528.
24. Wang CP, Li JL, Zhang LZ, Zhang XC, Yu S, Liang XM, et al. Isoquercetin protects cortical neurons from oxygen-glucose deprivation-reperfusion induced injury via suppression of TLR4-NF-κB signal pathway. Neurochem Int. 2013;63(8):741–9. doi:10.1016/j.neuint.2013.09.018.
25. Pan W, Li W, Wu H, Xie X, Xie M, Nie Q, et al. Aging-accelerated mouse prone 8 (SAMP8) mice experiment and network pharmacological analysis of aged liupao tea aqueous extract in delaying the decline changes of the body. Antioxidants. 2023;12(3):685. doi:10.3390/antiox12030685.
26. Hernández-Espinosa DR, Massieu L, Montiel T, Morán J. Role of NADPH oxidase-2 in the progression of the inflammatory response secondary to striatum excitotoxic damage. J Neuro Inflamm. 2019;16(1):91. doi:10.1186/s12974-019-1478-4.
27. Cinicola BL, Palumbo IM, Pannunzio A, Carnevale R, Bartimoccia S, Cammisotto V, et al. Low grade endotoxemia and oxidative stress in offspring of patients with early myocardial infarction. Antioxidants. 2023;12(4):958. doi:10.3390/antiox12040958.
28. Spina A, Guidarelli A, Buffi G, Fiorani M, Cantoni O. Unveiling the link between NADPH oxidase 2 activation and mitochondrial superoxide formation in leukemic cell killing induced by arsenic trioxide. Pharmacol Res. 2025;211(4):107554. doi:10.1016/j.phrs.2024.107554.
29. Münzel T, Templin C, Cammann VL, Hahad O. Takotsubo syndrome: impact of endothelial dysfunction and oxidative stress. Free Radic Biol Med. 2021;169(22):216–23. doi:10.1016/j.freeradbiomed.2021.03.033.
30. Zhang Y, Mao XD, Cao AL, Chu S, Li ZJ, Wang YM, et al. Astragaloside IV prevents endothelial dysfunction by improving oxidative stress in streptozotocin-induced diabetic mouse aortas. Exp Ther Med. 2021;22(5):1197.
31. Chi HJ, Chen ML, Yang XC, Lin XM, Sun H, Zhao WS, et al. Progress in therapies for myocardial ischemia reperfusion injury. Curr Drug Targets. 2017;18(15):1712–21. doi:10.2174/1389450117666160401120308.
32. Ibáñez B, Heusch G, Ovize M, Van de Werf F. Evolving therapies for myocardial ischemia/reperfusion injury. J Am Coll Cardiol. 2015;65(14):1454–71. doi:10.1016/j.jacc.2015.02.032.
33. Granger DN, Kvietys PR. Reperfusion injury and reactive oxygen species: the evolution of a concept. Redox Biol. 2015;6(508):524–51. doi:10.1016/j.redox.2015.08.020.
34. Tatar T, Polat Y, Comu FM, Kartal H, Arslan M, Kucuk A. Effect of cerium oxide on erythrocyte deformability in rat lower extremity ischemia reperfusion injury. Bratisl Lek Listy. 2018;119(7):441–3.
35. Drefs M, Thomas MN, Guba M, Angele MK, Werner J, Conrad M, et al. Modulation of glutathione hemostasis by inhibition of 12/15-lipoxygenase prevents ROS-mediated cell death after hepatic ischemia and reperfusion. Oxid Med Cell Longev. 2017;2017(1):8325754. doi:10.1155/2017/8325754.
36. Anderson SL, Singh B. Equine neutrophils and their role in ischemia reperfusion injury and lung inflammation. Cell Tissue Res. 2018;371(3):639–48. doi:10.1007/s00441-017-2770-1.
37. Hong X, Zhao X, Wang G, Zhang Z, Pei H, Liu Z. Luteolin treatment protects against renal ischemia-reperfusion injury in rats. Mediat Inflamm. 2017;2017(2):9783893. doi:10.1155/2017/9783893.
38. Fujii J, Homma T, Osaki T. Superoxide radicals in the execution of cell death. Antioxidants. 2022;11(3):501. doi:10.3390/antiox11030501.

39. Xiang M, Lu Y, Xin L, Gao J, Shang C, Jiang Z, et al. Role of oxidative stress in reperfusion following myocardial ischemia and its treatments. Oxid Med Cell Longev. 2021;1(1):6614009. doi:10.1155/2021/6614009.
40. Forde RC, Fitzgerald DJ. Reactive oxygen species and platelet activation in reperfusion injury. Circulation. 1997;95(4):787–9. doi:10.1161/01.cir.95.4.787.
41. Mohammadrezaei Khorramabadi R, Anbari K, Salahshoor MR, Alasvand M, Assadollahi V, Gholami M. Quercetin postconditioning attenuates gastrocnemius muscle ischemia/reperfusion injury in rats. J Cell Physiol. 2020;235(12):9876–83. doi:10.1002/jcp.29801.
42. Xu D, Hu MJ, Wang YQ, Cui YL. Antioxidant activities of quercetin and its complexes for medicinal application. Molecules. 2019;24(6):1123. doi:10.3390/molecules24061123.
43. Amić A, Lučić B, Stepanić V, Marković Z, Marković S, Dimitrić Marković JM, et al. Free radical scavenging potency of quercetin catecholic colonic metabolites: thermodynamics of $2H^+/2e^-$ processes. Food Chem. 2017;218(41):144–51. doi:10.1016/j.foodchem.2016.09.018.
44. Chen YW, Chou HC, Lin ST, Chen YH, Chang YJ, Chen L, et al. Cardioprotective effects of quercetin in cardiomyocyte under ischemia/reperfusion injury. Evid Based Complement Altern Med. 2013;2013:364519.
45. Ekinci Akdemir FN, Gülçin İ, Karagöz B, Soslu R, Alwasel SH. A comparative study on the antioxidant effects of hesperidin and ellagic acid against skeletal muscle ischemia/reperfusion injury. J Enzym Inhib Med Chem. 2016;31(s4):114–8. doi:10.1080/14756366.2016.1220378.
46. Zhao H, Lin X, Chen Q, Wang X, Wu Y, Zhao X. Quercetin inhibits the NOX2/ROS-mediated NF-κB/TXNIP signaling pathway to ameliorate pyroptosis of cardiomyocytes to relieve sepsis-induced cardiomyopathy. Toxicol Appl Pharmacol. 2023;477(38):116672. doi:10.1016/j.taap.2023.116672.
47. Sul OJ, Ra SW. Quercetin prevents LPS-induced oxidative stress and inflammation by modulating NOX2/ROS/NF-kB in lung epithelial cells. Molecules. 2021;26(22):6949. doi:10.3390/molecules26226949.
48. Wan H, Wang Y, Pan Q, Chen X, Chen S, Li X, et al. Quercetin attenuates the proliferation, inflammation, and oxidative stress of high glucose-induced human mesangial cells by regulating the miR-485-5p/YAP1 pathway. Int J Immunopathol Pharmacol. 2022;36:20587384211066440. doi:10.1177/20587384211066440.
49. Yousefi Zardak M, Keshavarz F, Mahyaei A, Gholami M, Moosavi FS, Abbasloo E, et al. Quercetin as a therapeutic agent activate the Nrf2/Keap1 pathway to alleviate lung ischemia-reperfusion injury. Sci Rep. 2024;14(1):23074. doi:10.1038/s41598-024-73075-7.
50. Sah MK, Gautam B, Pokhrel KP, Ghani L, Bhattarai A. Quantification of the quercetin nanoemulsion technique using various parameters. Molecules. 2023;28(6):2540. doi:10.3390/molecules28062540.
51. Cheng Y, Zhong C, Yan S, Chen C, Gao X. Structure modification: a successful tool for prodrug design. Future Med Chem. 2023;15(4):379–93. doi:10.4155/fmc-2022-0309.
52. Yu J, Fu R, Buhe A, Xu B. Quercetin attenuates lipopolysaccharide-induced hepatic inflammation by modulating autophagy and necroptosis. Poult Sci. 2024;103(6):103719. doi:10.1016/j.psj.2024.103719.
53. Jasenovec T, Radosinska D, Kollarova M, Balis P, Ferenczyova K, Kalocayova B, et al. Beneficial effect of quercetin on erythrocyte properties in type 2 diabetic rats. Molecules. 2021;26(16):4868. doi:10.3390/molecules26164868.